Bioorganic & Medicinal Chemistry Letters 20 (2010) 2163–2167

Contents lists available at ScienceDirect

Bioorganic & Medicinal Chemistry Letters

journal homepage: www.elsevier.com/locate/bmcl

Identification of pyridazino[4,5-*b*]indolizines as selective PDE4B inhibitors

Andrew F. Donnell [a,*], Paul J. Dollings [a,*], John A. Butera [a], Arlene J. Dietrich [a], Kerri K. Lipinski [b], Afshin Ghavami [b], Warren D. Hirst [b]

[a] *Worldwide Medicinal Chemistry, Pfizer Global Research and Development, CN 8000, Princeton, NJ 08543, USA*
[b] *Neuroscience Research Unit, Pfizer Global Research and Development, CN 8000, Princeton, NJ 08543, USA*

ARTICLE INFO

Article history:
Received 27 January 2010
Revised 8 February 2010
Accepted 8 February 2010
Available online 13 February 2010

Keywords:
Selective phosphodiesterase inhibitors
Pyridazino[4,5-*b*]indolizines
Hit-to-lead

ABSTRACT

Substituted pyridazino[4,5-*b*]indolizines were identified as potent and selective PDE4B inhibitors. We describe the structure–activity relationships generated around an HTS hit that led to a series of compounds with low nanomolar affinity for PDE4B and high selectivity over the PDE4D subtype.

Phosphodiesterase 4 (PDE4) is one of eleven PDE enzyme families responsible for the regulation of intracellular levels of cyclic adenosine monophosphate (cAMP) and cyclic guanosine monophosphate (cGMP).[1] PDE4 inhibition has been evaluated for the treatment of depressive disorders.[2] More recently, PDE4 inhibitors have been explored for treating a wider range of central nervous system (CNS) diseases including Parkinson's disease,[3] schizophrenia,[4] and Alzheimer's disease.[5] However, clinical studies of the PDE4 inhibitor rolipram were limited by side effects including nausea and emesis that were thought to arise from inhibition of the PDE4D subtype.[6] Similarly, side effects have restricted the therapeutic index of the second-generation PDE4 inhibitors cilomilast and roflumilast.[7] Selective inhibition of the PDE4B subtype may provide a means to achieve efficacy while potentially mitigating these adverse events.[8] Thus, we undertook a program directed toward the discovery of PDE4B-selective compounds. Recent reports highlighting chemotypes with varying levels of PDE4B selectivity illustrate the interest in such an approach.[9] Here, we report the discovery of pyridazino[4,5-*b*]indolizines as a novel class of potent and selective PDE4B inhibitors.

A high-throughput screen (HTS) of our in-house compound library identified the novel substituted pyridazino[4,5-*b*]indolizine **1**. This compound exhibited high affinity in our PDE4B binding assay (K_i = 2.60 μM), and it displayed 23-fold selectivity over PDE4D.[10] Comparable results were obtained from a cell-based adenylyl cyclase functional assay (PDE4B IC_{50} = 13.2 μM, PDE4D IC_{50} >100 μM).[11] Compound **1** also displayed reasonable biochemical and physicochemical lead-like properties. These factors prompted our use of **1** as a starting point in a hit-to-lead campaign aimed at improving the affinity for PDE4B while maintaining or elevating the level of selectivity over PDE4D. We targeted three of the major regions of **1** for synthetic explorations: (1) the pendant phenyl ring, (2) the pyrimidine tail-piece, and (3) the tricyclic pyridazino[4,5-*b*]indolizine core.

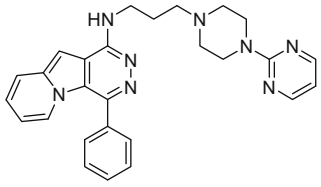

1
PDE4B K_i = 2.60 μM
PDE4D K_i = 59.0 μM
Selectivity (D/B) = 23

We designed a series of substituted-phenyl analogs to generate SAR around the phenyl ring. The most practical route for the synthesis of these compounds incorporated the diversity at an early stage, as shown in Scheme 1, by treatment of methyl indolizine-2-carboxylate (**2**) with the appropriate substituted benzoyl chlorides. Warming this mixture at 50 °C in the presence of base cleanly effected acylation of the 1-position of the indolizine. The resulting ketoesters **3a**–**f** were cyclized by condensation with hydrazine to provide, after chlorination with phosphorus oxychloride, the chloropyridazino[4,5-*b*]indolizines **4a**–**f**. The side chain

* Corresponding authors.
E-mail addresses: donnela@wyeth.com (A.F. Donnell), dollinp@wyeth.com (P.J. Dollings).

0960-894X/$ - see front matter © 2010 Elsevier Ltd. All rights reserved.
doi:10.1016/j.bmcl.2010.02.044

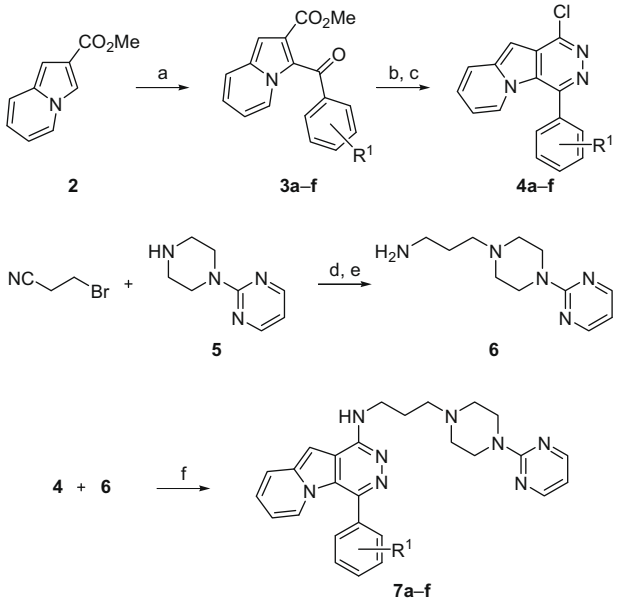

Scheme 1. Reagents and conditions: (a) $R^1C_6H_4COCl$, NaOAc, 50 °C; (b) hydrazine hydrate, EtOH, reflux; (c) $POCl_3$, reflux; (d) DMF, 60 °C; (e) H_2, Raney-Ni, 2 M NH_3–EtOH, rt; (f) NH_4Cl, NMP, 100 °C.

was constructed by alkylation of the piperazine **5** with 3-bromopropanenitrile, followed by reduction of the nitrile. The resulting amine **6** was introduced onto **4a–f** by nucleophilic aromatic substitution, giving the targeted compounds **7a–f**. Using similar chemistry, we also replaced the phenyl ring with heteroaromatic groups and various alkyl groups.

The analogs with substitution at the 2- and 4-positions of the phenyl ring had markedly lower PDE4B affinity. Likewise, replacement of the phenyl group with heteroaromatic groups and alkyl groups was not tolerated (data not shown). Substitution at the 3-position, particularly with electron-withdrawing groups, was tolerated. Selected compounds are displayed in Table 1. The methyl-substituted analog **7a** was somewhat less active than the lead **1**. Analogs containing a halogen (**7b–d**) were essentially equipotent with **1**, although PDE4B selectivity was eroded with the bromo and chloro species. The fluoro analog **7d** was the only compound that displayed modestly higher selectivity than **1**. Notably, the nitro-substituted analog **7f** showed a 10-fold increase in PDE4B binding affinity, but with a twofold decrease in selectivity.

Table 1
Substituted phenyl analogs

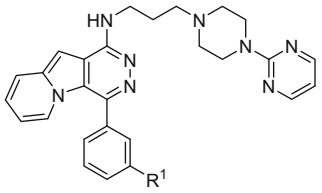

Compd	R^1	PDE4B K_i[a] (μM)	PDE4D K_i[a] (μM)	Selectivity[b] (D/B)
1	H	2.60	59.0	23
7a	Me	4.30 ± 2.77	54.4 ± 6.2	13
7b	Br	1.44 ± 0.65	17.5 ± 9.2	12
7c	Cl	2.01 ± 1.10	14.2 ± 2.9	7
7d	F	2.70 ± 1.14	83.0 ± 2.8	29
7e	CN	1.03 ± 0.38	3.35 ± 1.20	3
7f	NO_2	0.210 ± 0.099	2.40 ± 0.14	11

[a] Values that are the mean of two or more experiments are shown with their standard deviations.
[b] Ratio of K_i (PDE4D)/K_i (PDE4B).

We then examined the role of the pyrimidine tail-piece. Using an analogous synthetic pathway, we prepared several analogs with substitution on the pyrimidine. We also replaced the pyrimidine with other groups. All such changes significantly reduced the PDE4B activity (data not shown). Subsequently, we prepared an array of amide analogs as shown in Scheme 2. We elected to focus on the scaffold with the 3-fluorophenyl group because of its higher selectivity in the first round of SAR. Thus, introduction of an *N*-Boc-piperazine side chain onto the chloropyridazino[4,5-*b*]indolizine **4d**, followed by deprotection and acylation with a variety of acid chlorides, provided the amides **8a–g**.

The PDE4 binding results of this library are shown in Table 2. The acetamide **8a** retained the affinity of the lead, although this was attenuated with larger alkyl groups (**8b** and **8c**). The benzamide **8d** was tolerated, and the pyrrole amide **8e** was less active. Pyridyl groups (**8f**, **8g**) imparted sub-micromolar affinity and much greater selectivity.

Concurrently, we explored modifications of the core moiety, and developed the synthesis of a series of bicyclic pyrrolo[3,2-*d*]pyridazine analogs, in which the 'A-ring' of the lead tricycle has been truncated (Scheme 3). This synthesis commenced with the N-methylation of the known trisubstituted pyrrole **9**, which was prepared by the HCl-promoted cyclization of a ketonitrile.[12] Hydrogenolysis of the chloro group gave **10**. Regioselective lithiation of this species allowed for the introduction of substituted benzoyl groups at the 2-position. We included the moieties that had shown the most favorable activity in the tricyclic series. Cyclization of the resultant ketoesters **11a–d** to the pyrrolo[3,2-*d*]pyridazines **12a–d** was followed by installation of the side chain. This chemistry was performed analogously to that for the tricyclic analogs, providing the bicyclic analogs **13a–d**.

Pyrrolo[3,2-*d*]pyridazine **13a**, the direct bicyclic analog of the lead tricycle **1** exhibited 10-fold less affinity for PDE4B (Table 3). The loss of affinity was not as severe for the halogen- and nitro-substituted analogs **13b–d**, although they were slightly less active than their tricyclic comparators. In contrast to the tricyclic analogs, the bicycles, in particular the nitro species **13d**, displayed high levels of PDE4B-selectivity.

In a further iteration, we incorporated the pyridyl amide tail-pieces onto this scaffold and more exhaustively explored this motif with a variety of heteroaromatic amides. We retained the 3-nitrophenyl group in these studies because of the high PDE4B affinity and selectivity shown by **13d**. The synthesis of these compounds was carried out analogously to that described in Scheme 2 for the tricyclic species. We examined a range of amides, some of which are displayed in Table 4. Among pyridines, the 4-pyridyl isomer **14a** had reduced affinity, while the 3- and 2-pyridyl amides **14b** and **14c** displayed both high affinity and selectivity. Five-membered ring heterocycles (**14d–f**) showed varying levels of activity. Among diazines, the pyrazine amide **14h** showed the greatest affinity (77 nM) and also exhibited 58-fold selectivity over PDE4D.

We then returned to the original tricyclic scaffold with this optimized pyrazine amide tail-piece, and prepared the unsubsti-

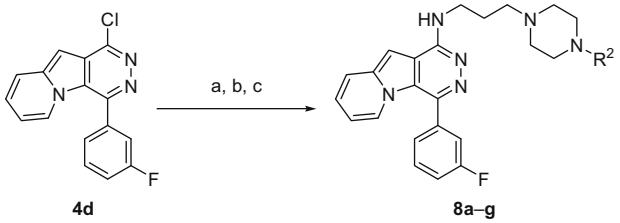

Scheme 2. Reagents and conditions: (a) *tert*-butyl 4-(3-aminopropyl)piperazine-1-carboxylate, NH_4Cl, NMP, 100 °C; (b) HCl–MeOH, 60 °C; (c) R^2COCl, *i*-Pr_2NEt, THF, 0 °C to rt.

Table 2
Piperazine amide analogs

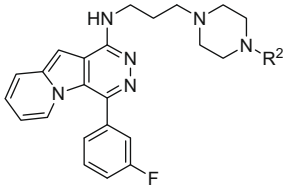

Compd	R^2	PDE4B K_i[a] (μM)	PDE4D K_i[a] (μM)	Selectivity[b] (D/B)
8a		1.90	>100	>53
8b		4.90	>100	>20
8c	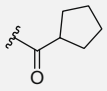	14.0	61.0	4
8d	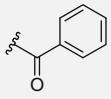	2.70	22.2	8
8e	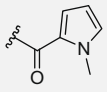	5.20	65.0	12
8f	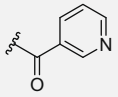	0.413	19.0	46
8g	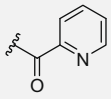	0.241	18.0	75

[a] Values are the result of one experiment.
[a] Ratio of K_i (PDE4D)/K_i (PDE4B).

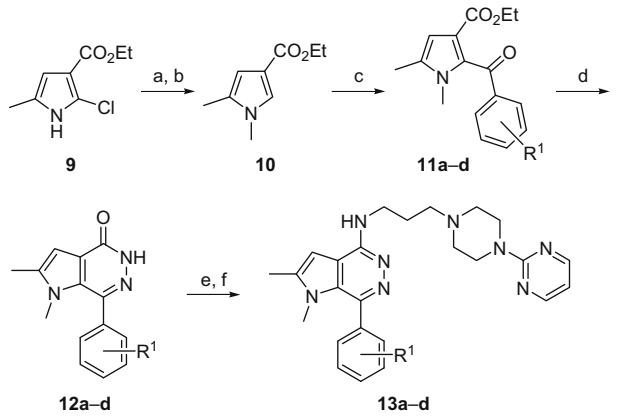

Scheme 3. Reagents and conditions: (a) KOH, EtOH, rt, then Me_2SO_4, acetone; (b) Pd-C, HCO_2NH_4, MeOH, rt; (c) *n*-BuLi, THF, −78 °C, then, when R^1 = H, Cl, or F: $R^1C_6H_4COCl$, or, when $R^1 = NO_2$: 3-NO_2–$C_6H_4C(O)N(OMe)Me$; (d) hydrazine hydrate, EtOH, rt; (e) $POCl_3$, reflux; (f) **6,** NH_4Cl, NMP, 100 °C.

tuted-phenyl analog **15**. This compound exhibited 41 nM PDE4B binding affinity and an impressive 205-fold selectivity over PDE4D (Table 5). By adding the 3-nitro substituent to the phenyl ring (**16**), we further increased the affinity to 5.6 nM, while sacrificing some of the selectivity gain. Selected compounds were examined in the functional, cell-based cAMP assay, but the potency did not always parallel the trends observed in the binding assay. The variations appeared to correlate with cell permeability, as measured by PAMPA. Despite this variability, the cyclase assay corroborated compound **16** as a potent and selective PDE4B inhibitor (PDE4B IC_{50} = 0.389 μM, PDE4D IC_{50} = 4.90 μM).[13] We further profiled **16** for selectivity against other PDEs and did not observe any significant activity against these targets (PDEs 1–3, 5, and 6: IC_{50} >10 μM). Likewise, compound **16** was selective for PDE4B

Table 3
Bicyclic analogs

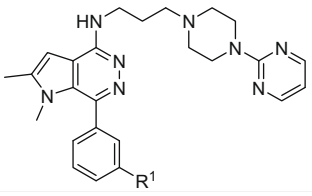

Compd	R^1	PDE4B K_i[a] (μM)	PDE4D K_i[a] (μM)	Selectivity[b] (D/B)
13a	H	26.2	>100	>4
13b	Cl	5.50 ± 2.97	80.9 ± 33.0	15
13c	F	4.40 ± 0.42	>100	>24
13d	NO_2	1.00	>100	>100

[a] Values that are the mean of two or more experiments are shown with their standard deviations.
[b] Ratio of K_i (PDE4D) / K_i (PDE4B).

Table 4
Bicyclic analogs with piperazine amides

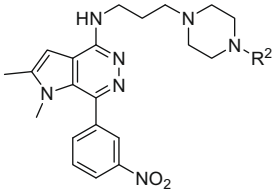

Compd	R^2	PDE4B K_i[a] (μM)	PDE4D K_i[a] (μM)	Selectivity[b] (D/B)
14a	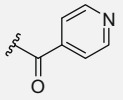	52.2	>100	>2
14b	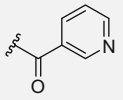	0.432	15.3	35
14c	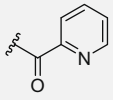	0.238	11.5	48
14d	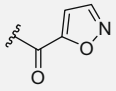	5.08	>100	>20
14e	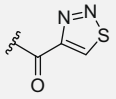	0.977	48.6	50
14f	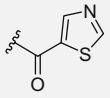	0.222	12.7	57
14g	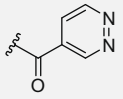	4.44	51.2	12
14h	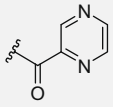	0.077 ± 0.013	4.44 ± 0.06	58

[a] Values that are the mean of two or more experiments are shown with their standard deviations.
[b] Ratio of K_i (PDE4D)/K_i (PDE4B).

Table 5
Pyrazine amide analogs

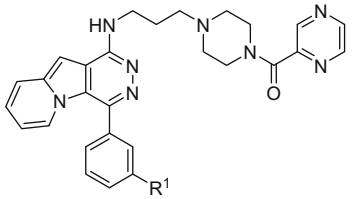

Compd	R^1	PDE4B K_i[a] (μM)	PDE4D K_i[a] (μM)	Selectivity[b] (D/B)
15	H	0.041 ± 0.009	8.37 ± 2.33	205
16	NO_2	0.0056 ± 0.0001	0.147 ± 0.004	26

[a] Values that are the mean of two or more experiments are shown with their standard deviations.
[b] Ratio of K_i (PDE4D)/K_i (PDE4B).

versus the PDE4A and PDE4C subtypes (>fivefold selectivity in the cyclase assay). Subsequent characterization of these compounds found that they inhibit hERG channels. Additionally, compound **16** had poor oral bioavailability in PK studies. Nevertheless, these compounds are potentially valuable tools for understanding the structural features responsible for PDE4B selectivity.

In summary, we have identified a series of novel, potent, PDE4B-selective pyridazino[4,5-*b*]indolizines. By utilizing the results of SAR studies around HTS hit **1**, we prepared compound **15**, which exhibited >200-fold selectivity for PDE4B over PDE4D, and, in compound **16**, we produced a species with single-digit nanomolar affinity for PDE4B.

Acknowledgments

We thank the management of the Neuroscience and Medicinal Chemistry departments for their support of this program.

References and notes

1. (a) Houslay, M. D.; Schafer, P.; Zhang, K. Y. J. *Drug Discovery Today* **2005**, *10*, 1503; (b) Bender, A. T.; Beavo, J. A. *Pharmacol. Rev.* **2006**, *58*, 488.
2. (a) Wachtel, H. *Neuropharmacology* **1983**, *22*, 267; (b) Przegalinski, E.; Bigajska, K. *Pol. J. Pharmacol. Pharm.* **1983**, *35*, 233; (c) Zhang, H.-T. *Curr. Pharm. Des.* **2009**, *15*, 1688.

3. Yang, L.; Calingasan, N. Y.; Lorenzo, B. J.; Beal, M. F. *Exp. Neurol.* **2008**, *211*, 311.
4. (a) Millar, J. K.; Pickard, B. S.; Mackie, S.; James, R.; Christie, S.; Buchanan, S. R.; Malloy, M. P.; Chubb, J. E.; Huston, E.; Baillie, G. S.; Thomson, P. A.; Hill, E. V.; Brandon, N. J.; Rain, J.-C.; Camargo, L. M.; Whiting, P. J.; Houslay, M. D.; Blackwood, D. H. R.; Muir, W. J.; Porteous, D. J. *Science* **2005**, *310*, 1187; (b) Kanes, S. J.; Tokarczyk, J.; Siegel, S. J.; Bilker, W.; Abel, T.; Kelly, M. P. *Neuroscience* **2007**, *144*, 239; (c) Siuciak, J. A.; Chapin, D. S.; McCarthy, S. A.; Martin, A. N. *Psychopharmacology* **2007**, *192*, 415.
5. (a) Rose, G. M.; Hopper, A.; De Vivo, M.; Tehim, A. *Curr. Pharm. Des.* **2005**, *11*, 3329; (b) Ghavami, A.; Hirst, W. D.; Novak, T. J. *Drugs R. D.* **2006**, *7*, 63; (c) Blokland, A.; Schreiber, R.; Prickaerts, J. *Curr. Pharm. Des.* **2006**, *12*, 2511; (d) McLachlan, C. S.; Chen, M. L.; Lynex, C. N.; Goh, D. L. M.; Brenner, S.; Tay, S. K. H. *Arch. Neurol.* **2007**, *64*, 456; (e) Reneerkens, O. A. H.; Rutten, K.; Steinbusch, H. W. M.; Blokland, A.; Prickaerts, J. *Psychopharmacology* **2009**, *202*, 419.
6. Robichaud, A.; Stamatiou, P. B.; Jin, S.-L. C.; Lachance, N.; MacDonald, D.; Laliberté, F.; Liu, S.; Huang, Z.; Conti, M.; Chan, C.-C. *J. Clin. Invest.* **2002**, *110*, 1045.
7. Spina, D. *Br. J. Pharmacol.* **2008**, *155*, 308.
8. Srivani, P.; Usharani, D.; Jemmis, E. D.; Sastry, G. N. *Curr. Pharm. Des.* **2008**, *14*, 3854.
9. (a) Huang, Z.; Liu, S.; Zhang, L.; Salem, M.; Greig, G. M.; Chan, C. C.; Natsumeda, Y.; Noguchi, K. *Life Sci.* **2006**, *78*, 2663; (b) Giovannoni, M. P.; Cesari, N.; Graziano, A.; Vergelli, C.; Biancalani, C.; Biagini, P.; Piaz, V. D. *J. Enzyme Inhib. Med. Chem.* **2007**, *22*, 309; (c) Kranz, M.; Wall, M.; Evans, B.; Miah, A.; Ballantine, S.; Delves, C.; Dombroski, B.; Gross, J.; Schneck, J.; Villa, J. P.; Neu, M.; Somers, D. O. *Bioorg. Med. Chem.* **2009**, *17*, 5336; (d) Naganuma, K.; Omura, A.; Maekawara, N.; Saitoh, M.; Ohkawa, N.; Kubota, T.; Nagumo, H.; Kodama, T.; Takemura, M.; Ohtsuka, Y.; Nakamura, J.; Tusjita, R.; Kawasaki, K.; Yokoi, H.; Kawanishi, M. *Bioorg. Med. Chem. Lett.* **2009**, *19*, 3174.
10. Inducible CHO cells stably expressing β2 adrenergic receptor and either PDE4B3 or PDE4D4 were seeded at 6×10^7 cells in a 10-cell factory (Corning) in Ham's F12 medium, 10% FBS, 100 units penicillin streptomycin and induced with 50 nM mifepristone for 48 h before harvesting. Cell pellets were lysed in 50 ml Ripa buffer (50 mM Tris, pH 7.5, 20 mM NaCl, and 1% NP40) for 15 min on ice. Particulate matter was removed by centrifugation at 27,000*g* for 1 h at 4 °C. The supernatant was aliquoted and frozen at −20 °C until use in assay. Compounds were diluted to a final concentration ranging from 100 μM to 0.3 nM. Each assay well contained 200 μl of diluted lysate, 25 μl of diluted compound, and 25 μl of [methyl-^{3}H]-rolipram (2.5 nM final). Plates were incubated at 30 °C for 1 h with gentle rotation. The reaction was terminated by filtering with ice-cold assay buffer (10 mM Tris, pH 7.5 and 50 mM $MgCl_2$) on a GF/B filter mat using a Filtermate harvester (Packard). Plates were dried at 37 °C for 1 h and then counted on a TopCount liquid scintillation counter (Packard). CPM values were expressed as percent specific binding and plotted against compound concentration. A curve was fitted using a four-parameter logistic fit and the IC_{50} value was determined. The K_i was calculated using the Cheng–Prusoff equation, $pK_i = IC_{50}/(1+L/K_d)$, where L is the concentration of free radioligand used in the assay and K_d is the dissociation constant of the radioligand for the receptor. The IC_{50} is the concentration of competing ligand that displaces 50% of the specific binding of the radioligand.
11. Inducible CHO cells stably expressing β2 adrenergic receptor and either PDE4B3 or PDE4D4 were plated at 2×10^4 cells/well in 96-well plates in Ham's F12 medium, 10% FBS, 100 units penicillin streptomycin and induced with 50 nM mifepristone for 48 h before use in assay. Media was removed from cells and replaced with serum-free Ham's F12 medium and incubated at 37 °C for 15 min. Compounds were diluted to a final concentration ranging from 100 μM to 0.3 nM. Isoproterenol (10 μM final) was added to compound wells. Controls included four wells each of Ham's F12 medium alone, isoproterenol alone, and 10 μM rolipram with isoproterenol. Cells were incubated at 37 °C for 15 min, then 100 mM perchloric acid was added to stop the reaction and lyse cells for a minimum of 15 min. In Optiplates (Packard), 50 μl of cell lysate was added per well, plus 50 μl each of [^{125}I]-cAMP, primary rabbit cAMP antibody, and SPA PVT fluomicrospheres with anti-rabbit secondary-antibody according to manufacturer's directions. Plates were incubated at room temperature overnight and then read on a TopCount liquid scintillation counter (Packard).
12. Foley, L. H. *Tetrahedron Lett.* **1994**, *35*, 5989.
13. For compound **15**, the PDE4B IC_{50} was 6.7 μM in the cyclase assay. We were unable to determine an accurate value for selectivity against PDE4D due to limitations of the assay at higher concentrations (IC_{50} >100 μM).